JOURNAL OF Applied Polymer SCIENCE

Increasing Solvent Polarity and Addition of Salts Promote β-Phase Poly(vinylidene fluoride) Formation

Yuen Kei Adarina Low, Li Yi Tan, Lay Poh Tan, Freddy Yin Chiang Boey, Kee Woei Ng
School of Materials Science and Engineering, Nanyang Technological University, Singapore 639798, Singapore
Correspondence to: K. W. Ng (E-mail: kwng@ntu.edu.sg)

ABSTRACT: This article investigates the effects of solvent polarity and salt addition on β-phase poly(vinylidene fluoride) (PVDF) formation. Films were solvent cast in aprotic solvents of varying polarities with or without salt addition. Characterization was done by Fourier transformed infra-red spectroscopy, differential scanning calorimetry, and scanning electron microscopy. Decreasing fractions of β-phase PVDF was observed with increasing drying temperature when less polar solvents were used. The most polar solvent (hexamethylphosphoramide) consistently produced films with at least 90.0% β-phase PVDF within the crystalline regions. Melting temperatures increased in correlation to absolute proportions of β-phase PVDF. Salt addition increased the formation of β-phase PVDF by 30%, with salts of higher valencies and smaller ionic radii resulting in more significant increases. Taken collectively, using solvents of higher polarities and addition of salts with high cationic valencies and small ionic radii will maximize β-phase formation in solvent cast PVDF films. © 2012 Wiley Periodicals, Inc. J. Appl. Polym. Sci. 000: 000–000, 2012

KEYWORDS: films; biomaterials; morphology

Received 30 June 2012; accepted 7 August 2012; published online
DOI: 10.1002/app.38451

INTRODUCTION

Poly(vinylidene fluoride) (PVDF) exists in at least four polymorphs (α, β, γ, and δ) that give rise to varying net dipole moments across the polymer chains.[1,2] Among the polymorphs, β-phase PVDF possesses the strongest dipole moment lateral to the chain axis, resulting in significant piezoelectric properties.[3,4] This makes β-phase PVDF particularly interesting in applications such as microelectromechanical systems, sensors, and actuators.[5,6] More recently, PVDF also attracted attention as a biomaterial because of its biostability, lower bending stiffness, and ability to evoke minimal host tissue response.[7] Results from our earlier study further suggested that varying cellular responses can be induced by different PVDF polymorphs.[8] To deepen our understanding on PVDF polymorphs toward cellular behavior, we aim to fabricate films with controlled and known β-phase for evaluation.

A number of reports on fabrication strategies to induce higher proportion of β-phase PVDF are available.[9–12] Although solvent casting using different solvents in the presence of salts has been suggested, mechanical stretching remains the most direct and is, therefore, popular.[2,13] However, mechanical stretching can result in undesirable structural deformations that may affect the application.[14] Better understanding of the influence of solvents and salts in β-phase PVDF formation could, therefore, help to prevent this. Several polar solvents have been demonstrated to favor the production of β-phase PVDF films fabricated by solvent casting,[11,15,16] but results have been controversial due to a lack of consistency in casting conditions.

Increased percentages of β-phase PVDF have also been reported after salt addition,[14,17,18] but the mechanism for this is unclear. Yoon et al. suggested that interactions of cationic salts, in their case Ca^{2+}, toward the carbonyl oxygen of dimethylformaldehyde (DMF) induced electropositive and negative ends, thereby resulting in PVDF orientating and aligning in the all-trans β-phase arrangement.[14] Indeed, affinity of the electronegative carbonyl oxygen in DMF toward cations from inorganic salts was observed using infrared spectroscopy.[19,20] Phadke et al. concluded that higher electronic cloud density around the cationic salt induced a red shift in C=O stretching in DMF solvent, which can be correlated to stronger solvent-salt interaction.[20] It was further suggested that the presence of large anions will create steric hindrance for solvent-cationic salt interactions toward electropositive nitrogen atom in DMF.[20,21] Thus, the electronic cloud density of cations and ionic radii ratios of anions to cations will together influence the magnitude of stretching frequency and result in higher proportions of β-phase PVDF.[19,20] However, the salts used in these studies had variations in cationic sizes and valencies which may have confounded the results. Besides addition of salt, several strategies have also been developed in favor of the growth of β-phase PVDF. The addition of nanoparticles or fillers and hydrated salts can also increase the formation of polar phases by

Table I. Conditions for Synthesizing PVDF Films after Dissolution in Solvent According to the $N + (N - 1)$ Method of Titration[26]

	Drying duration (min)			Drying temperature (°C)			Casting thickness (mm)		
Condition	30	60	90	60	100	140	0.3	0.5	0.7
1	*					*		*	
2		*				*		*	
3			*			*		*	
4		*		*				*	
5		*			*			*	
6		*				*	*		
7		*				*			*

Asterisks stand for conditions for PVDF film fabrication.

inducing interactions between the negatively charged entities and dipole moments of PVDF.[22–24] In the same principle, improved miscibility of polyelectrolyte/polymer blends also favors the formation of the β-phase PVDF.[25]

Despite observations that solvent polarity and the presence of salts influenced the proportion of β-phase PVDF obtained, there is limited understanding of the chemical mechanisms of these phenomena. In this study, we, therefore, attempted to systemically compare the effects of solvents and salts on β-phase PVDF formation, while keeping other fabrication conditions constant. The first objective of this work was to characterize the effect of four aprotic solvents with different properties on the fraction of β-phase, degree of crystallinity, and surface morphology of PVDF films synthesized under various conditions. This allows a basis to understand the mechanism of β-phase PVDF formation in solvents of different polarities.

The second objective was to profile the influence of different chloride salts on β-phase PVDF formation. In this aspect, we hypothesized that ionic charge and size play a direct role in influencing the fraction of β-phase PVDF formed in solvent cast films. Therefore, we evaluated the effects of adding chloride salts with different cationic valencies at three concentrations, on the fraction of β-phase, degree of crystallinity, and surface morphology of PVDF films.

EXPERIMENTAL

PVDF Films Fabrication with Solvent of Varying Polarities and Properties

Dimethylacetamide (DMAc, 3.72D, Aldrich), *N, N*-dimethylformamide (DMF, 3.86D, Tedia), *N*-methyl-2-pyrrolidone (NMP, 4.09D, Tedia), and hexamethylphosphoramide (HMPA, 5.54D, Aldrich) were used to dissolve as-received PVDF homo-polymer (Solef®, Solvay Solexis) at 10–90 (w/v) %. Following dissolution, PVDF films were synthesized by solvent casting at three drying durations (30, 60, and 90 min), drying temperatures (60°C, 100°C, and 140°C), and casting thicknesses (0.3, 0.5, and 0.7 mm). The "$N + (N - 1)$" method[26] was used to titrate these three casting parameters (Table I). Films were immersed in 95% technical grade ethanol (Aik Moh Paints and Chemical) for 24 h to remove residual solvents after cooling down to room temperature in the oven.

PVDF Films Fabrication with Salt Addition

Sodium chloride (NaCl, Lab-Scan Analytical Science), potassium chloride (KCl, Analar BDH), magnesium chloride ($MgCl_2$, Sigma), and calcium chloride ($CaCl_2$, Merck) salts were mixed at 1, 3, and 5% (w/w) with PVDF homo-polymer before dissolution into DMF solvent at 10–90% (w/v). PVDF films were solvent cast onto glass substrates with wet thickness 0.5 mm and dried for 1 week at room conditions before characterization.

Characterization of Synthesized PVDF Films

Short-range molecular arrangements of PVDF molecules were validated using Fourier transform infrared spectroscopy (FTIR, PerkinElmer Spectrum GX) set at the following parameters: range 400–1000 cm^{-1}, resolution 1 cm^{-1}, diaphragm diameter 1 cm. Dry thicknesses of films were measured with a micrometer gauge at five random points. Mean thicknesses were used for calculating the fraction of β-phase PVDF present within the crystalline regions of the films [$F(\beta)$], using a method first described by Osaki and Ishida.[8,27] Thermal properties were measured using differential scanning calorimetry (DSC, TA Instrument Q10) at a heating rate of 10°C/min from 100 to 200°C. Degree of crystallinity obtained from DSC results was used to calculate the absolute proportion of β-phase PVDF (%β) within the crystalline region of each film, represented by the following equation:

$$\%\beta = F(\beta)x \text{ degree of crystallinity} \quad (1)$$

Thermal gravimetric analysis (TGA) was used to determine the percentage of residual solvent after film drying. Surface morphology was assessed by scanning electron microscopy (SEM) after 80 s gold sputtering at 18 mA. The SEM micrographs were taken at 3.0 kV, spot size 40–50.

Statistics

All statistical analyses were carried out using IBM SPSS Statistics 19 software. Results were analyzed for statistical significance using one-way analysis of variance (ANOVA) with 95% confidence interval and Tukey's post-test for multiple comparisons. *P* values less than 0.05 were considered to be significant.

RESULTS

Quantification of β-Phase PVDF in Solvent Cast Films

Using the "$N + (N - 1)$" method of titration,[26] the relationship between casting conditions (drying duration, drying temperature,

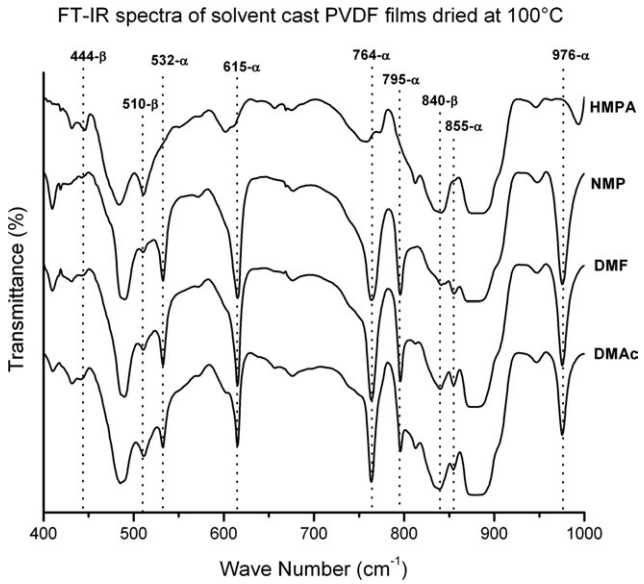

Figure 1. FTIR spectra of PVDF films cast with increasing solvent polarities at 100°C. α-Phase peaks (532 cm^{-1}, 615 cm^{-1}, 764 cm^{-1}, 795 cm^{-1}, 855 cm^{-1}, and 976 cm^{-1}) were absent in HMPA-PVDF film, whereas β-phase peaks (444 cm^{-1}, 510 cm^{-1}, and 840 cm^{-1}) were observed. α-Phase peaks dominated NMP, DMF, and DMAc-PVDF films, although β-phase peaks were also noted.

and casting thickness) and fraction of β-phase [$F(\beta)$] in PVDF films were established for the four solvents used. While only β-phase peaks were observed for HMPA synthesized PVDF (HMPA-PVDF), FTIR spectra of all other three solvent cast PVDF films dried at 100°C showed a mixture of α- and β-phase peaks (Figure 1). Among them, DMAc-PVDF had notable β-phase peaks at 510 cm^{-1} and 840 cm^{-1}, whereas the most prominent α-phase peaks were observed for NMP-PVDF at 615 cm^{-1} and 976 cm^{-1}.

The graphs of $F(\beta)$ against various PVDF synthesizing conditions showed that $F(\beta)$ was dependent of the polarity of solvents but independent on drying duration or casting thickness [Figure 2(a, b)]. Drying temperature exerted the greatest influence on $F(\beta)$ among the three casting parameters studied. In general, increasing drying temperature resulted in decreasing $F(\beta)$. Statistical analysis showed significant differences in $F(\beta)$ between PVDF films cast from the different solvents at 60°C and 100°C drying temperatures ($P < 0.05$; ANOVA and Tukey's test). At 140°C, $F(\beta)$ values for HMPA-PVDF were at least 90.0%, whereas the rest were significantly lower, at values between 12.5% and 16.1% [Figure 2(c)].

The highest mean $F(\beta)$ value of 53.3% was recorded for NMP-PVDF at the drying temperature of 60°C, whereas a drastic drop to 11.3% was observed when drying temperature was increased to 100°C. No further increase in $F(\beta)$ was observed upon further increase in drying temperature of NMP-PVDF to 140°C. An equally significant drop in $F(\beta)$ value, from 82.7% to 44.6%, was recorded for DMAc-PVDF as drying temperature was increased from 60°C to 100°C. This dropped further to 16.1% when drying temperature was raised to 140°C. The sharpest drop in $F(\beta)$ value from 91.7% to 21.8% was recorded for DMF-PVDF when drying temperature was increased from 60°C and 100°C. This value slide further to 12.5%, the lowest $F(\beta)$ value recorded for all solvent cast PVDF films at this condition. Our results suggest that drying temperatures and $F(\beta)$ values in PVDF films were inversely related when DMAc, DMF, and NMP were used as solvents.

HMPA-PVDF could not be produced at drying temperature of 60°C because complete drying could not be achieved over the drying duration of 60 min used in this study. At all other conditions used, the $F(\beta)$ values for HMPA-PVDF were consistently at least 90%. Drying at 100°C and 140°C yielded $F(\beta)$ of 90.0% and 93.1%, respectively, suggesting that the high polarity of

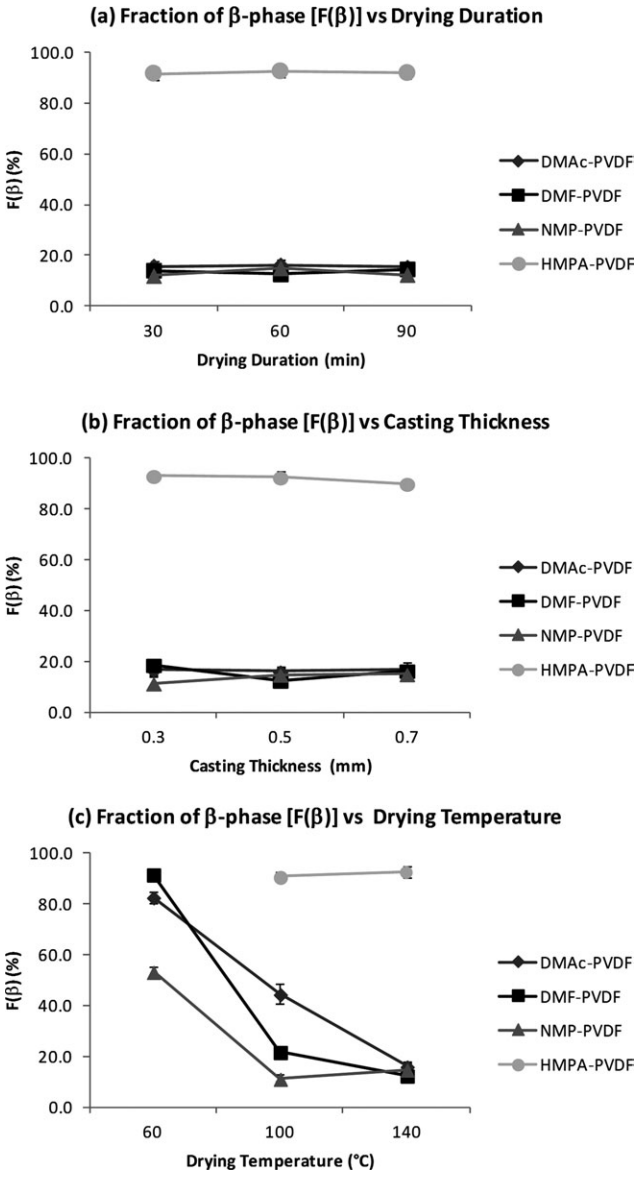

Figure 2. Calculated fraction of β-phase over increasing (a) drying duration (at drying temperature of 140°C), (b) casting thickness (at drying temperature of 140°C), and (c) drying temperature. Increasing drying temperature influenced the fraction of β-phase PVDF formation significantly.

HMPA could be the dominant factor responsible for the high $F(\beta)$ of HMPA-PVDF films within the range of parameters evaluated.

Melting Temperature and Crystallinity of PVDF Films

DSC results showed that the melting temperature (T_m) of PVDF films varied with the solvent used. The mean T_m of HMPA-PVDF was the highest compared with other solvent-cast PVDF films. Specifically at the drying temperature of 140°C, DMAc-PVDF recorded the lowest mean T_m, of 170.9°C, whereas HMPA-PVDF had the highest mean T_m of 174.5°C, which was significantly higher than the other groups [Figure 3(a)].

The degree of crystallinity for all samples fluctuated in the range of 41.0–50.9%. No significant differences were observed for PVDF films cast with the different solvents ($P > 0.05$; ANOVA and Tukey's test), suggesting minimal effect of solvent polarity on crystallinity [Figure 3(b)]. The plot of mean degree of crystallinity against %β showed that crystallinity did not change significantly with increasing absolute amounts of β-phase PVDF, indicating no correlation between the two parameters [Figure 3(c)].

When DSC and FTIR results were taken collectively, a linearly increasing correlation between T_m and %β for the three less polar solvents was observed. However, no significant difference was concluded statistically. Only HMPA-PVDF films showed significantly higher T_m and %β at the drying temperature of 140°C.

Surface Morphology of PVDF Films

Surface morphology of PVDF films was analyzed via SEM imaging of the top surfaces which were exposed to air during the casting process. Spherulites were evident on most sample surfaces but their sizes and distribution were not always homogeneous. Randomly distributed pores at spherulite boundaries were also observed on some samples (Figures 4 and 5). No significant trends were observed in the surface topographies and spherulite sizes of films subjected to different drying duration (data not shown). However, the spherulite sizes of DMF-PVDF, DMAc-PVDF, and NMP-PVDF increased with increasing drying temperatures (Figure 4). In these three groups, smaller spherulite size, typically less than 1.5 μm in diameter, corresponded to higher $F(\beta)$ values of 82.7% and above [Figure 4(a1,b1)], whereas larger spherulite size, occasionally in excess of 30 μm in diameter, corresponded to lower $F(\beta)$ values of 16.1% and below [Figure 4(b3,c3)]. At 100°C and 140°C drying temperatures, spherulite sizes increase in the order DMF < DMAc < NMP, corresponding to increasing boiling temperatures. Spherulite morphology was less defined in HMPA-PVDF samples (Figure 5), with surface undulations appearing as large grains in the sample dried at 100°C [Figure 5(a)]. In contrast to the other three groups, increasing drying temperature to 140°C induced significantly smaller surface grains/spherulites that are covered with submicron pores distributed all over the film surface [Figure 5(b)].

Quantification of β-Phase PVDF in Films Solvent Cast with Salts

PVDF films were cast in DMF and dried at room condition over a 1 week period to evaluate the influence on β-phase formation in the presence of chloride salts. The assortment of

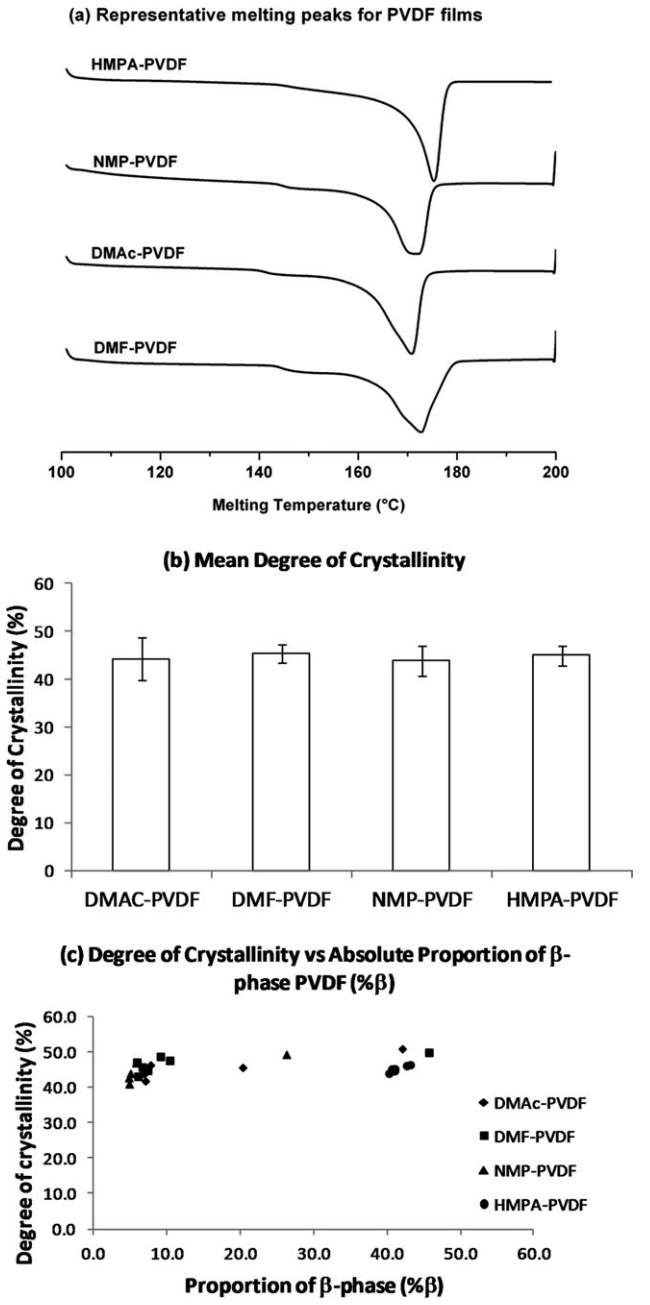

Figure 3. Comparison of melting temperature and crystallinity across the four solvents used. (a) DSC profiles showing mean melting temperatures (T_m) of PVDF films synthesized at the drying temperature of 140°C. HMPA synthesized PVDF films (HMPA-PVDF) recorded significantly higher T_m compared with the rest. (b) Mean degree of crystallinity of all four solvent cast PVDF films showed no significant differences at the drying temperature of 140°C ($P > 0.05$). (c) Fluctuations in the degree of crystallinity were minimal, over increasing %β.

mono and divalent salts was chosen to assess the influence of ionic size and charge on β-phase PVDF formation. Films synthesized without salt but under the same drying conditions were used as controls. Addition of 1 wt % NaCl, KCl, $MgCl_2$, and $CaCl_2$ distinctly weakened the characteristic α-phase peaks in corresponding FT-IR spectrums (data not shown), and raised

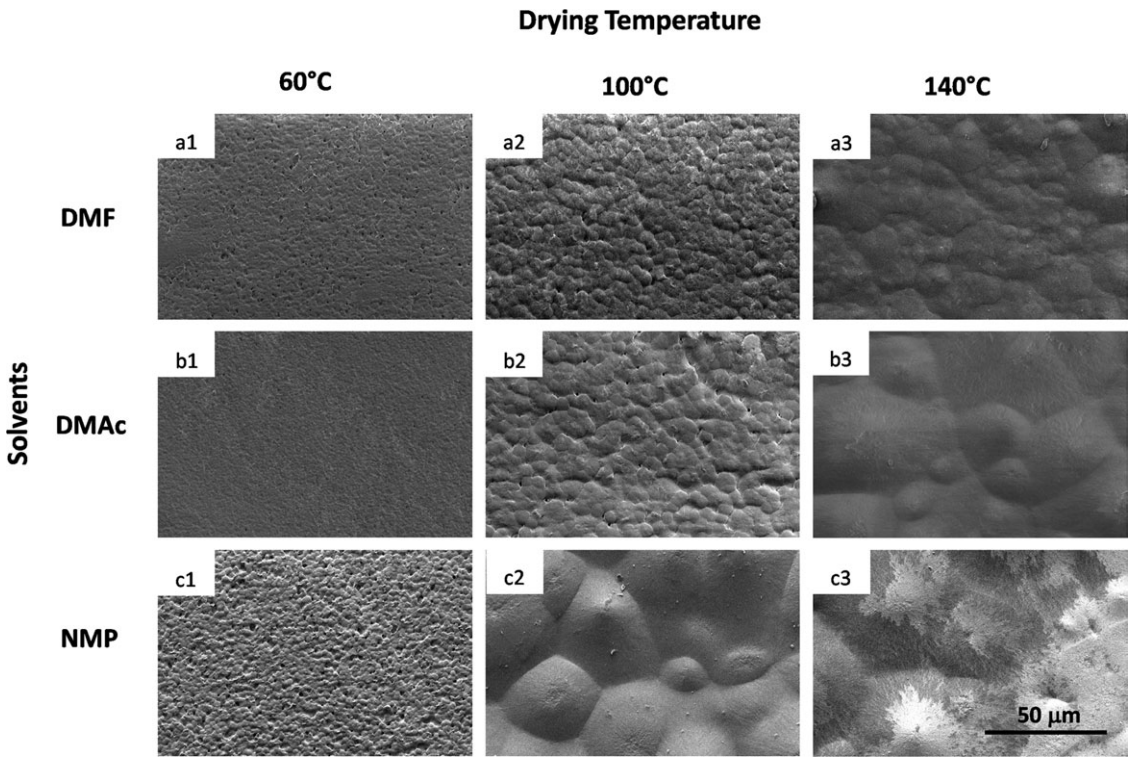

Figure 4. Scanning electron microscopy images of (a1–a3) DMF-PVDF, (b1–b3) DMAc-PVDF, and (c1–c3) NMP-PVDF. Films were dried at 60°C, 100°C, and 140°C for 60 min. Increasing spherulite size was observed with increasing drying temperatures for DMF-PVDF, DMAc-PVDF, and NMP-PVDF.

the calculated mean $F(\beta)$ values to 93.1%, 88.4%, 95.8%, and 94.9%, respectively, compared with 64.4% in controls ($P < 0.01$). $F(\beta)$ values of DMF-PVDF cast in the presence of KCl was found to be significantly lower than all other groups at all weight percentages [$P < 0.05$; Figure 6(a)]. From the same graph, it was observed that increasing salt concentration did not significantly increase $F(\beta)$ values, regardless of salt type. However, $F(\beta)$ values decreased with increasing ionic radii [ionic radii arranged in descending order: K^+ (1.38 Å), Na^+ (1.02 Å), Ca^{2+} (0.99 Å), Mg^{2+} (0.72 Å)[28]].

Mean melting temperatures were not statistically different from control when salt was added (data not shown). Likewise, increasing salt concentration from 1 wt % to 5 wt % did not change T_m significantly for each salt type. However, T_m of films cast in NaCl was lower than in the other salt types, although this was statistical significant only when compared with $MgCl_2$ and $CaCl_2$ at 3 wt %. Although the mean degree of crystallinity of control films dried at room temperature (59.6%) was significantly higher than films dried at 60°C (49.8%), 100°C (47.6%), and 140°C (47.1%), addition of any of the chloride salts did not result in significant changes in the degree of crystallinity. The absolute proportion of β-phase (%β) was calculated to be above 51.5% for all salt types at all concentrations studied. This percentage was higher than any HMPA-PVDF films, which had the highest proportion of β-phase among films synthesized without the addition of salts.

Surface Morphology of PVDF Films Solvent Cast with Salts

Surfaces of all films with salt addition at all concentrations were rough, porous, and void of spherulites. Increasing salt

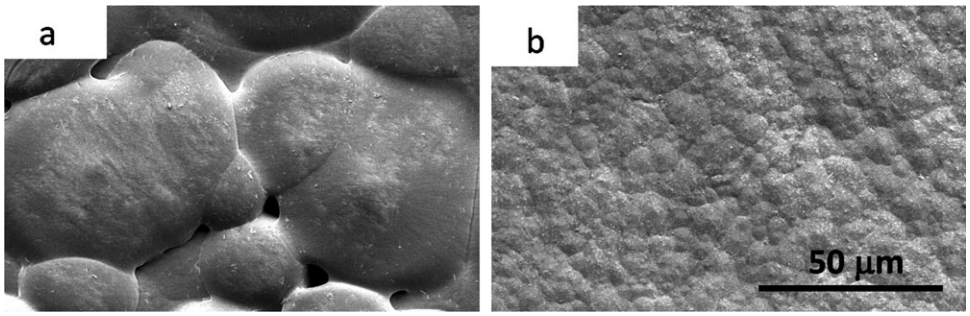

Figure 5. Spherulite morphology of HMPA-PVDF samples dried at (a) 100°C and (b) 140°C. Spherulite size at 140°C was significantly smaller, and covered with submicron pores as compared with films dried at 100°C.

Applied Polymer SCIENCE

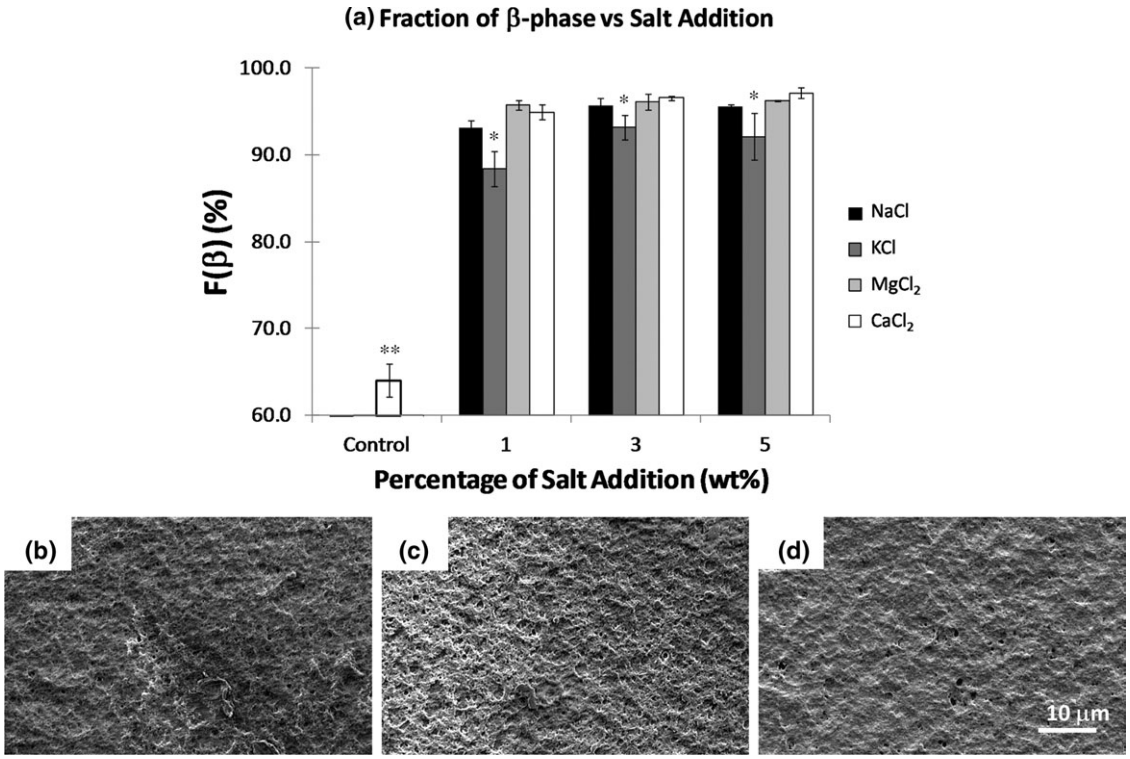

Figure 6. Variation of the (a) fraction of β-phase PVDF [$F(\beta)$] and representative SEM images of PVDF films cast in DMF, in the presence of (b) 1 wt %, (c) 3 wt %, and (d) 5 wt % salt. All films were cast in DMF with a wet thickness of 0.5 mm and dried at room condition over 1 week. $F(\beta)$ of control films (without addition of salt) were significantly lower than all groups with salt addition ($^{**}P < 0.01$). Addition of KCl at all three percentages gave lower $F(\beta)$ compared with other salt types ($^{*}P < 0.05$). Surfaces were rough, porous, and void of spherulites. All the salt types produced similar film surfaces over the concentrations used.

concentrations from 1 wt % to 5 wt % showed no increase in pore densities or change in topography for all salt types [Figure 6(b–d)].

DISCUSSION

Solution casting is the technique chosen for fabricating β-phase PVDF films in our work. It is preferred over spin casting and electrospinning due to the ease of obtaining uniform micrometer thick films using a calibrated doctor blade. Even though spin-coat films were reported to have enhanced β-phase formation, it is limited to fabrication of nano-scaled thickness films, which only allow evaluation of the surface properties for bulk applications. It will be interesting to obtain micron-scale thickness films with α-phase and polar β-phase directly from solution casting technique, due to its advantages in easy manufacturing and downstream modifications.

The first step for fabricating PVDF films using any techniques described previously is solvation. Solvation is the formation of chemical bonds between a solvent and solute. The solution stability is consequently influenced by hydrogen bonds, dipole moments, and solvent polarities. In our attempt to correlate solvent properties to β-phase PVDF formation, four aprotic solvents with different boiling temperatures [DMF (153°C), DMAc (165°C), NMP (203°C), HMPA (232°C)], polarities [DMAc (3.72D), DMF (3.86D), NMP (4.09D), HMPA (5.54D)], and structures were used for casting. Our findings suggest that drying duration and casting thickness have minimal effects, whereas drying temperature exerted the most significant influence on the fraction of β-phase PVDF [$F(\beta)$] formed using each of the four solvents. This is in contrast to results presented by Cardoso et al., where thinner films produced on a spin coater gave rise to increased β-phase PVDF.[29] However, in spin coating, polymers were stretched in all directions of a plane. It was reported that the extension of molecular chain during high-speed rotation and subsequent crystallization can freeze the PVDF chain in its extended β-phase morphology.[30] The speed of spin coating, solution viscosity, humidity, and temperatures influenced the percentage of β-phase in PVDF, but with controversies because the complete processing conditions were often not mentioned.[31] Similarly, electro spinning also stretch the polymers, but uniaxially. The end product of an electrospun sample consists of nanofibers with diameters in the order of several hundred nanometers, making up meshes of interlocking β-phase fibers with high porosity.

The solvents used in our study had different structures and dipole moments. These differences alter the local conformation around the carbonyl oxygen atom, which influenced the steric effect in aprotic solvents.[32] The high polarity of HMPA is a result of the higher incidences of polar N—P and O=P bonds. As a consequence, more electrostatic interactions between the PVDF molecular chains and HMPA accelerate the rate of

dissolution, favoring the formation of trans-state β-phase PVDF. The lower solvent evaporation rate of HMPA further enhanced this effect because the extended duration of drying due to its higher boiling point, favors the formation of the thermodynamically stable β-phase PVDF, in agreement with existing literature.[1] Despite that, TGA analysis confirmed a negligible percentage of residual HMPA-PVDF samples after ethanol immersion (data not shown).

Although DMAc and DMF solvents have lower boiling temperatures and polarities among the four aprotic solvents, denoting higher evaporation rate at the same drying temperature, $F(\beta)$ values of DMAc-PVDF and DMF-PVDF films were higher than NMP-PVDF at drying temperatures of 60°C and 100°C [Figure 2(c)]. This can be explained by the local bulkiness of NMP molecules that played a role in solvation steric effects.[32] Steric hindrance due to the cyclic structure of NMP molecules prevented effective electrostatic interactions with PVDF, thereby discouraging the formation of polar polymorphs, evidenced by low $F(\beta)$ values in NMP-PVDF samples. In this aspect, influence of steric hindrance on PVDF polymorph formation was more dominant than solvent polarity at 60°C. The drop in $F(\beta)$ value for NMP-PVDF when drying temperature was increased to 100°C suggests that the higher rate of evaporation resulted in more randomized phase formation. This was also reflected by the lower degree of crystallinity.

Drying below 70°C is known to favor the synthesis of β-phase PVDF. At the relatively lower drying temperature of 60°C in our experiment, the higher polarity of DMF compared with DMAc allowed stronger electrostatic interactions between DMF and PVDF in comparison with DMAc and PVDF. The stronger electrostatic interactions in turn overwhelmed the contribution of evaporation rates in determining conformational phases, depicted by the higher $F(\beta)$ value in DMF-PVDF. When drying temperature was increased to 100°C, the higher rate of evaporation of DMF compared with DMAc fixed the PVDF chains in metastable and amorphous states, resulting in a lower $F(\beta)$ value for DMF-PVDF. As crystal perfection determines the melting temperature,[33] we observed slightly higher melting temperatures for DMAc-PVDF than DMF-PVDF films dried at 60°C, although this was not statistically significant.

Crystal perfection and total degree of crystallinity will collectively determine the melting temperature.[33] The variations of T_m between the four PVDF groups could be correlated to the absolute amounts of α- and β-phase PVDF present.[34] Specifically, higher T_m has been attributed to β-phase PVDF while lower T_m to α-phase PVDF,[35] an observation that we also made in our earlier study.[8] Indeed, our current data for HMPA produced films at all tested conditions also showed significantly higher melting temperature for higher absolute proportion of β-phase. However, similar observations could not be made for PVDF produced by the three less polar solvents.

When effort was made to fabricate as high a concentration of α-phase PVDF as possible, spherulitic structures of average diameter 50 μm were observed.[30] Gregorio and de Souza Nociti showed that increasing drying temperature up to 140°C resulted in larger PVDF spherulites (12 μm in diameter) due to the maximum crystallization rate occurring close to 145°C, when NMP and HMPA solvents were used.[1,36] Congruent to this, we observed increased spherulite sizes in DMF-PVDF, DMAc-PVDF, and NMP-PVDF with increasing drying temperature from 60 to 140°C (Figure 4), but a decline in $F(\beta)$. Interestingly, this trend was reversed in our results for HMPA-PVDF (Figure 5), presumably due to the dominant effects of high polarity and high boiling temperature of HMPA. To the best of our knowledge, the reason for this difference has not been reported, but a lower rate of evaporation at any particular drying temperature would have given the spherulites time to grow. In addition, cooling rate will also affect spherulite sizes.[37] In our case, because all the PVDF films were allowed to cool to room temperature in the oven after drying at the stipulated temperatures, we assumed similar cooling rates for films dried at the same temperature. It was documented that HMPA formed its peroxide readily when exposed to oxygen and light.[38] However, there are no reports on the effect of HMPA peroxide toward polymer dissolution to date.

In our study, monovalent and divalent chloride salts were used to determine their effects on the formation of β-phase in PVDF films dried at room conditions. Our findings suggested that $F(\beta)$ was more significantly affected by the salt type rather than salt concentration. Longer duration of drying combined with addition of salt significantly increased the $F(\beta)$. In addition, the value of $F(\beta)$ decreased with increasing ionic radii of cation. Enhanced ion-dipole interaction could also potentially induce a larger fraction of β-phase PVDF.[39] Stronger electronic clouds around divalent Mg^{2+} and Ca^{2+} compared with monovalent Na^+ and K^+ consequently result in higher strengths of interaction between the divalent cations and the resonant structures of DMF molecules. Ion-dipole interactions between the cation and carbonyl O encourage arrangement of PVDF chains into trans-state β-phase, with the alignment of electronegative fluorine atoms on one side of the PVDF carbon backbone (Figure 7). As a result, higher $F(\beta)$ values were recorded in PVDF films made in the presence of $MgCl_2$ and $CaCl_2$, compared with KCl [Figure 6(a)]. However, this difference was not observed when compared with the NaCl group. Lower ionic radii ratio of NaCl compared with KCl caused stronger ion-dipole interaction between Na^+ and the carbonyl O, comparable with the divalent salts. Therefore, higher $F(\beta)$ values were recorded in the NaCl group compared with the KCl group at all concentrations tested. Similar observations of increased formation in β-phase PVDF had also been reported with the addition of onium salts.[40] It was suggested that the onium salts acted as nucleating agents, resulting in the formation of spherulites of 7 μm diameter with the addition of 1% onium salt. In agreement with our data [Figure 6(b–d)], addition of onium salts also resulted in PVDF surfaces that were rough, porous, and without distinct spherulite boundaries. It is also worthy to note that PVDF films produced without salt but dried at room temperature resulted in an increase in $F(\beta)$ up to 64.4%. This may be related to the fact that β-phase PVDF is favored thermodynamically and kinetically at this drying condition. The long duration for evaporation favored the formation of higher amounts of β-phase PVDF.

It had been demonstrated that addition of NaCl from 0 to 6 wt % resulted in an increase followed by a decrease in the degree

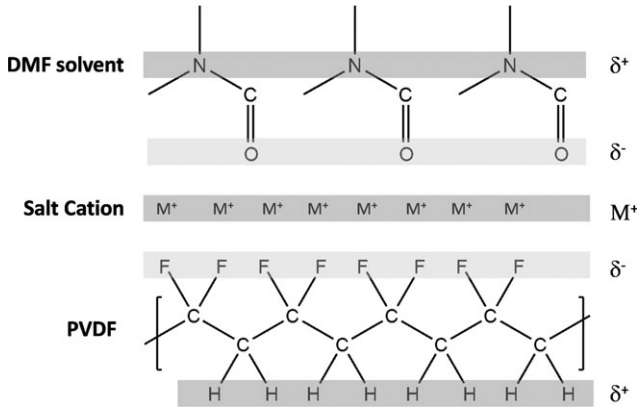

Figure 7. Model of DMF-salt-PVDF interaction. Using a monovalent cation (M^+) as an example, carbonyl oxygen atoms ($\delta-$) of DMF interact electrostatically with the salt cations ($\delta+$) to induce an all-trans β-phase orientation of PVDF molecules.

of crystallinity of PVDF, cast in DMF dried over 7 days at 50°C.[41] The postulation was that when NaCl was added in minute amounts, the salt combined with free radicals near the crystallite surfaces to increase crystalline volume. However, beyond a critical percentage of NaCl, excess salt will interact with PVDF on the crystallite surfaces to dislocate the atoms, resulting in a fall in the degree of crystallinity. Our results showed that the degree of crystallinity in the salt-added PVDF films (between 55.5% and 62.6%) was higher than in PVDF synthesized without salt addition, dried at 60°C, 100°C, or 140°C. Although the degree of crystallinity was higher with salt addition, crystal structures may not be perfect, resulting in lower T_m.[33] Environmental humidity during the drying process could also affect the crystallization process,[11,42,43] and the relative humidity in our drying condition was between 55 and 65%. Addition of hydrated salt was also shown to promote nucleation and crystallization of β-phase, although the exact mechanism of that is unclear.[17,42] It was suggested that the hydrogen bonding between the water molecules stored in hydroscopic salt and polar C—F bonds of PVDF was responsible for the β-phase formation. Because DMF is a hygroscopic solvent, we postulate that water molecules in the atmosphere interact with DMF and PVDF molecules via hydrogen bonding when the PVDF films were left to dry in atmospheric conditions for 1 week, in this study. The small proportion of α-phase PVDF after salt addition may be attributed to the presence of free DMF and self-associated DMF molecules that do not form salt-DMF complexes.[44] In this case, PVDF chains will be randomly organized, thus preferentially forming the kinetically favorable α-phase polymorph.

Taken collectively, cations present in the solvent-PVDF mixtures will have an affinity toward the electronegative fluorine atoms along the PVDF chains and the carbonyl oxygen in DMF, thereby favoring the formation of β-phase PVDF.

CONCLUSIONS

In this study, we characterized the effects of using four aprotic solvents with different polarities and addition of chloride salts on β-phase PVDF formation in solvent cast films. Our results revealed that solvent type and drying temperature influenced the fraction of β-phase PVDF while the duration of drying and casting thickness did not. Specifically, HMPA which has the highest polarity among the four solvents studied, consistently produced films with at least 90.0% β-phase PVDF within the crystalline regions, regardless of other casting parameters. The other solvents with relatively lower polarity produced decreasing fractions of β-phase PVDF with increasing drying temperature. Melting temperature increased with increasing absolute proportion of β-phase PVDF. An absolute β-phase PVDF proportion of about 40% was associated with melting temperatures of about 174°C, whereas an absolute β-phase PVDF proportion of less than 20% was associated with melting temperature of about 171°C. Spherulite size observed on PVDF film surfaces increased with increasing drying temperatures in all groups except those cast in HMPA, where the reversed was observed.

The fractions of β-phase PVDF increased with the addition of NaCl, KCl, $MgCl_2$, and $CaCl_2$ salts during casting, to levels comparable with HMPA cast films. However, increasing salt concentration from 1 wt % to 5 wt % did not translate into significantly higher fractions of β-phase. Salts that produced cations of higher charge or smaller cationic size resulted in higher fraction of β-phase produced, supporting our hypothesis that ionic charges and size can influence the fraction of β-phase PVDF formation.

REFERENCES

1. Gregorio, R.; Borges, D. S. *Polymer* **2008,** *49*, 4009.
2. Imamura, R.; Silva, A. B.; Gregorio, R. *J. Appl. Polym. Sci.* **2008,** *110*, 3242.
3. Lovinger, A. *J. Science* **1983,** *220*, 1115.
4. Mohammadi, B.; Yousefi, A. A.; Bellah, S. M. *Polym. Test* **2007,** *26*, 42.
5. Lu, X.; Li, S. K.; Xu, Z.; Ren, W.; Cheng, Z. Y. *Ferroelectrics* **2010,** *409*, 78.
6. Oh, S. R.; Yao, K.; Chow, C. L.; Tay, F. E. H. *Thin Solid Films* **2010,** *519*, 1441.
7. Klinge, U.; Klosterhalfen, B.; Ottinger, A. P.; Junge, K.; Schumpelick, V. *Biomaterials* **2002,** *23*, 3487.
8. Low, Y. K. A.; Meenubharathi, N.; Niphadkar, N. D.; Boey, F. Y. C.; Ng, K. W. *J. Biomater. Sci. Polym. Ed.* **2010,** *22*, 1651.
9. Lin, D.-J.; Chang, C.-L.; Huang, F.-M.; Cheng, L.-P. *Polymer* **2003,** *44*, 413.
10. Ma, W. Z.; Zhang, J.; Wang, X. L. *J. Mater. Sci.* **2008,** *43*, 398.
11. Salimi, A.; Yousefi, A. A. *J. Polym. Sci. Part B: Polym. Phys.* **2004,** *42*, 3487.
12. Sathanon, U.; Fukura, S.; Sekiguchi, A.; Ogino, K.; Miyata, S. *J. Appl. Polym. Sci.* **2004,** *92*, 856.
13. Mhalgi, M. V.; Khakhar, D. V.; Misra, A. *Polym. Eng. Sci.* **2007,** 47, 1992.
14. Yoon, S.; Prabu, A. A.; Kim, K. J.; Park, C. *Macromol. Rapid Commun.* **2008,** *29*, 1316.

15. Benz, M.; Euler, W. B. *J. Appl. Polym. Sci.* **2003,** *89*, 1093.
16. He, X. J.; Yao, K. *Appl. Phys. Lett.* **2006,** *89*, 112909.
17. He, X.; Yao, K.; Gan, B. K. *Sens. Actuators A* **2007,** *139*, 158.
18. Tawansi, A.; Oraby, A. H.; Abdelrazek, E. M.; Abdelaziz, M. *Polym. Test* **1999,** *18*, 569.
19. Du, J. M.; Zhang, X. W. *J. Appl. Polym. Sci.* **2008,** *109*, 2935.
20. Phadke, M. A.; Musale, D. A.; Kulkarni, S. S.; Karode, S. K. *J. Polym. Sci. Part B: Polym. Phys.* **2005,** *43*, 2061.
21. Waghorne, W. E.; Rubalcava, H. *J. Chem. Soc. Faraday Trans. 1* **1982,** *78*, 1199.
22. Lopes, A. C.; Costa, C. M.; Tavares, C. J.; Neves, I. C.; Lanceros-Mendez, S. *J. Phys. Chem. C* **2011,** *115*, 18076.
23. Sencadas, V.; Martins, P.; Pitaes, A.; Benelmekki, M.; Ribelles, J. L. G.; Lanceros-Mendez, S. *Langmuir* **2011,** *27*, 7241.
24. Yu, L.; Cebe, P. *Polymer* **2009,** *50*, 2133.
25. Gibon, C. M.; Norvez, S.; Tence-Girault, S.; Goldbach, J. T. *Macromolecules* **2008,** *41*, 5744.
26. Sun, T. T. *Nat. Rev. Mol. Cell Biol.* **2004,** *5*, 577.
27. Osaki, S.; Ishida, Y. *J. Polym. Sci. Part B: Polym. Phys.* **1975,** *13*, 1071.
28. Barbalace, K. *Periodic Table of Elements—Sorted by Ionic Radius. EnvironmentalChemistry.com*; 1995–2011; Available at: http://EnvironmentalChemistry.com/yogi/periodic/ionicradius.html. [Updated 1995–2012 2/22/2007; Cited 24/04/2012].
29. Cardoso, V. F.; Minas, G.; Costa, C. M.; Tavares, C. J.; Lanceros-Mendez, S. *Smart Mater Struct.* **2011,** *20*, 087002.
30. Sencadas, V.; Gregorio, R.; Lanceros-Mendez, S. *J. Macromol. Sci. Part B: Phys.* **2009,** *48*, 514.
31. Ramasundaram, S.; Yoon, S.; Kim, K. J.; Lee, J. S. *Macromol. Chem. Phys.* **2008,** *209*, 2516.
32. Zhang, Y.; Watanabe, N.; Umebayashi, Y.; Ishiguro, S.-i. *J. Mol. Liq.* **2005,** *119*, 167.
33. Prest, W. M., Jr.; Luca, D. J. *J. Appl. Phys.* **1975,** *46*, 4136.
34. Sencadas, V.; Lanceros-Mendez, S.; Mano, J. F. *Thermochim. Acta* **2004,** *424*, 201.
35. Salimi, A.; Yousefi, A. A. *Polym. Test* **2003,** *22*, 699.
36. Gregorio, R.; de Souza Nociti, N. C. *J. Phys. D: Appl. Phys.* **1995,** *28*, 432.
37. Langkammerer, C. M.; Catlin, W. E. *J. Polym. Sci.* **1948,** *3*, 305.
38. Jose, J.; Hytte, J. M.; Cléchet, P. *J. Chem. Thermodyn.* **1973,** *5*, 857.
39. Nandi, P. K.; Sannigrahi, A. B. *THEOCHEM—J. Mol. Struct.* **1994,** *113*, 99.
40. Vijayakumar, R. P.; Khakhar, D. V.; Misra, A. *J. Polym. Sci. Part B: Polym. Phys.* **2011,** *49*, 1339.
41. Elashmawi, I. S. *Cryst. Res. Technol.* **2007,** *42*, 389.
42. Benz, M.; Euler, W. B.; Gregory, O. *J. Macromolecules* **2002,** *35*, 2682.
43. Grubb, D. T.; Choi, K. W. *J. Appl. Phys.* **1981,** *52*, 5908.
44. Kabisch, G.; Kálmán, E.; Pálinkás, G.; Radnai, T.; Gaizer, F. *Chem. Phys. Lett.* **1984,** *107*, 463.